



ELSEVIER

Journal of Alloys and Compounds 330–332 (2002) 141–145

Journal of  
ALLOYS  
AND COMPOUNDS

www.elsevier.com/locate/jallcom

## Hexagonal $\text{LaNiSnD}_2$ with a filled ZrBeSi-type structure

V.A. Yartys<sup>a,\*</sup>, T. Olavesen<sup>a,b</sup>, B.C. Hauback<sup>a</sup>, H. Fjellvåg<sup>b</sup>, H.W. Brinks<sup>a</sup><sup>a</sup>Institute for Energy Technology, P.O. Box 40, N-2027 Kjeller, Norway<sup>b</sup>Department of Chemistry, University of Oslo, N-0315 Oslo, Norway

### Abstract

$\text{LaNiSnD}_2$  dideuteride was synthesised and characterised by powder synchrotron X-ray and neutron diffraction and thermal desorption spectroscopy. Transformation from orthorhombic  $\text{TiNiSi}$  into the hexagonal ZrBeSi type proceeds in the metal sublattice upon deuteration. In  $\text{LaNiSnD}_2$  (space group  $P6_3/mmc$ ;  $a = 4.42249(4)$ ,  $c = 8.67405(9)$  Å) deuterium atoms completely occupy one type of  $\text{La}_3\text{Ni}$  tetrahedra, sharing common vertexes and edges and forming a spatial framework. The shortest interatomic distances in the structure are: La–D, 2.6118(4) Å; Ni–D, 1.619(2) Å; Sn–D, 2.718(2) Å; and D–D, 2.780(2) Å. Reversible formation of  $\text{LaNiSn}$  from the deuteride proceeds in vacuum at 670 K, with a peak of D evolution at 530–610 K. © 2002 Elsevier Science B.V. All rights reserved.

**Keywords:** Lanthanum nickel tin deuteride; Powder neutron diffraction; Synchrotron X-ray diffraction; Thermal desorption spectroscopy

### 1. Introduction

The intermetallic compound  $\text{LaNiSn}$  is a constituent of the  $\text{LaNi}_{5-x}\text{Sn}_x$  ( $x = 0.2\text{--}0.5$ ) alloys, which are promising materials for advanced nickel–metal hydride batteries [1]. It crystallises in the orthorhombic  $\text{TiNiSi}$ -type structure [2–4]. This is the most frequently observed structure type for the equiatomic RTX (R, rare earth metal; T, transition metal; X, nontransition element) ternaries [5]. Despite the abundance of  $\text{TiNiSi}$ -based intermetallics, no crystal structure studies of their corresponding hydrides have been reported so far.

The present study focused on the hydrogen absorption–desorption properties of  $\text{LaNiSn}$  and the crystal structure of the saturated deuteride  $\text{LaNiSnD}_2$ .

### 2. Experimental

The  $\text{LaNiSn}$  alloy was prepared by argon arc melting of mixtures of high-purity lanthanum (99.9%), nickel (99.9%) and tin (99.9%). The alloy specimen was homogenised by annealing at 770 K for 4 weeks. Powder X-ray diffraction (PXD) data [Siemens D5000 diffractometer,  $\text{Cu K}\alpha_1$  radiation, Bragg Brentano geometry, position sensitive detector and synchrotron PXD at SNBL,

ESRF] confirmed the formation of  $\text{LaNiSn}$  with the orthorhombic  $\text{TiNiSi}$ -type structure. The refined unit cell parameters,  $a = 7.6827(2)$ ,  $b = 4.6616(1)$ ,  $c = 7.6071(2)$  Å, agree well with the reference data [2–4]. No significant impurities were found in the sample. Deuteration of  $\text{LaNiSn}$  was performed at 670 K at a deuterium loading pressure of 1 bar. The synthesis resulted in the formation of the stoichiometric dideuteride  $\text{LaNiSnD}_2$ .

Powder neutron diffraction (PND) data were collected between  $2\theta = 10.00$  and  $130.00^\circ$  in steps of  $\Delta(2\theta) = 0.05^\circ$  at 298 K with the two-axis powder diffractometer PUS at the JEEP II reactor, Kjeller, Norway ( $\lambda = 1.5554$  Å, focusing Ge (511) monochromator, position sensitive detectors). A rotating cylindrical vanadium sample holder with 5 mm inner diameter was used. Synchrotron (SR) PXD data were obtained at the Swiss Norwegian Beam Line (BM 1) at ESRF, Grenoble, France. Data were collected between  $2\theta = 3.00$  and  $31.38^\circ$  in steps of  $\Delta(2\theta) = 0.005^\circ$  at 298 K (Debye–Scherrer mode,  $\lambda = 0.49868$  Å, channel-cut Si (111) monochromator). The sample was kept in a rotating glass capillary of diameter 0.3 mm.

The structure of  $\text{LaNiSnD}_2$  was solved by combined Rietveld-type refinements of the PXD (SR) and the PND data sets using the GSAS program package [6]. The nuclear scattering lengths  $b_{\text{La}} = 8.24$ ,  $b_{\text{Ni}} = 10.30$ ,  $b_{\text{Sn}} = 6.23$  and  $b_{\text{D}} = 6.67$  fm and the X-ray form factor coefficients were taken from the GSAS library. The peak profiles were modelled using a pseudo-Voigt function.

\*Corresponding author. Tel.: +47-63-806-453; fax: +47-63-810-920.  
E-mail address: volodymyr.yartys@ife.no (V.A. Yartys).

Cosine Fourier series polynomials were used to model the background of both data sets.

The thermal desorption spectroscopy studies were performed in dynamic vacuum at pressures not exceeding  $6 \times 10^{-5}$  mbar. A constant heating rate of  $2^\circ/\text{min}$  was used heating from room temperature to 870 K.

### 3. Results and discussion

The PXD (SR) pattern of  $\text{LaNiSnD}_2$  can be indexed on the basis of both orthorhombic ( $a = 8.6741(1)$ ,  $b = 4.4230(2)$ ,  $c = 7.6592(3)$  Å) and hexagonal ( $a = 4.42249(4)$ ,  $c = 8.67405(9)$  Å) unit cells. The formation of the  $\text{LaNiSnD}_2$  deuteride from  $\text{LaNiSn}$  is accompanied by a rather strong anisotropic lattice expansion ( $\Delta a/a = 12.9\%$ ,  $\Delta b/b = -5.1\%$ ,  $\Delta c/c = 0.7\%$ ), implying a rather modest increase of the unit cell volume ( $\Delta V/V = 7.9\%$ ). The anisotropic distortion results in a  $c/b$  ratio for the orthorhombic cell of 1.7317, close to the ideal value of  $\sqrt{3}$  for a hexagonal unit cell. A simple relation between the metric constants,  $a_{\text{hex}} \sim b_{\text{orth}} \sim c_{\text{orth}}/\sqrt{3}$  and  $c_{\text{hex}} \sim a_{\text{orth}}$ , exists for these two settings (see Table 1 for further details). Consideration of the  $\text{TiNiSi}$  type as an orthorhombically deformed hexagonal  $\text{ZrBeSi}$ -type structure (superstructure to the  $\text{AlB}_2$  type) is well established and documented in the

literature (e.g. Ref. [5]). Based on the refined unit cell parameters, the transformation of the metal sublattice from orthorhombic  $\text{TiNiSi}$  into an hexagonal  $\text{ZrBeSi}$ -type structure can be suggested upon deuteration.

The PXD (SR) data show no indication of diffraction line splitting (full width at half maximum of the peaks is typically  $0.025^\circ$  in  $2\theta$ ). No significant differences were observed in the refinements with the 'orthorhombic' and 'hexagonal' settings for the structure of  $\text{LaNiSnD}_2$ . Further combined refinements based on the PXD (SR) and PND data sets gave no significant improvement in the fit using the orthorhombic setting, despite the increased number of variable positional parameters for the orthorhombic structure (10) compared to the hexagonal (1) (see Table 1 for details). Hence, the hexagonal setting is used for the description of the  $\text{LaNiSnD}_2$  deuteride.

The observed, calculated and difference PND and PXD (SR) profiles are shown in Fig. 1.

In the hexagonal structure of  $\text{LaNiSnD}_2$  the deuterium atoms completely occupy a single  $\text{La}_3\text{Ni}$  tetrahedral site. The occupied interstices are connected by vertexes and edges and form a spatial framework (Fig. 2).

$\text{LaNiSn}$  is characterised by distorted trigonal prisms  $\text{La}_6$  with Sn and Ni, respectively, at their centres giving  $\text{SnLa}_6$  and  $\text{NiLa}_6$  polyhedra (Fig. 3a). Sn and Ni form a buckled  $\text{Sn}_3\text{Ni}_3$  network (Fig. 4). The formation of  $\text{LaNiSnD}_2$

Table 1  
Relations between the orthorhombic and hexagonal descriptions of the crystal structure of  $\text{LaNiSnD}_2$

	Orthorhombic setting	Hexagonal setting
Structure type of the metal sublattice	$\text{TiNiSi}$	$\text{ZrBeSi}$
Space group	$Pnma$ (No. 62)	$P6_3/mmc$ (No. 194)
Unit cell dimensions (Å)	$a = 8.6741(1)$ $b = 4.4230(2)$ $c = 7.6592(3)$	$a = 4.42249(4)$ $c = 8.67405(9)$
Metric relations for the unit cells	$a_{\text{orth}}$ $b_{\text{orth}}$ $c_{\text{orth}}$	$c_{\text{hex}}$ $a_{\text{hex}}$ $a_{\text{hex}}\sqrt{3}$
Orthorhombicity parameter, $\delta^a$	$2.2 \times 10^{-4}$	—
No. of positional parameters	10	1
Atoms and their coordinates <sup>b</sup>	4 La in 4c: 0.9995(6), 1/4, 0.7473(4) 4 Ni in 4c: 0.2544(6), 1/4, 0.4177(9) 4 Sn in 4c: 0.2424(4), 1/4, 0.0780(7) 3.96(6) D1 in 4c: 0.9331(10), 1/4, 0.0966(22) 4.00(–) D2 in 4c: 0.5597(10), 1/4, 0.0873(23)	2 La in 2a: 0, 0, 0 2 Ni in 2c: 1/3, 2/3, 1/4 2 Sn in 2d: 2/3, 1/3, 1/4 4.00(–) D in 4f: 1/3, 2/3, 0.4365(3)
Reliability factors	$R_{\text{pr}} = 0.040$ (PND) $R_{\text{wpr}} = 0.054$ (PND) $R_{\text{pr}} = 0.055$ (PXD(SR)) $R_{\text{wpr}} = 0.082$ (PXD(SR))	$R_{\text{pr}} = 0.042$ (PND) $R_{\text{wpr}} = 0.057$ (PND) $R_{\text{pr}} = 0.058$ (PXD(SR)) $R_{\text{wpr}} = 0.085$ (PXD(SR))

$$^a \delta = 1 - c_{\text{orth}}/b_{\text{orth}}\sqrt{3}.$$

<sup>b</sup> The crystal structure of the initial  $\text{LaNiSn}$  intermetallic compound reveals mixed occupancy of Ni and Sn in two 4c sites with the sequence between Ni and Sn in these sites of, respectively, 9:1 and 1:9. This sequence was confirmed and fixed during the final refinements of the data for  $\text{LaNiSnD}_2$  in both orthorhombic and hexagonal settings.

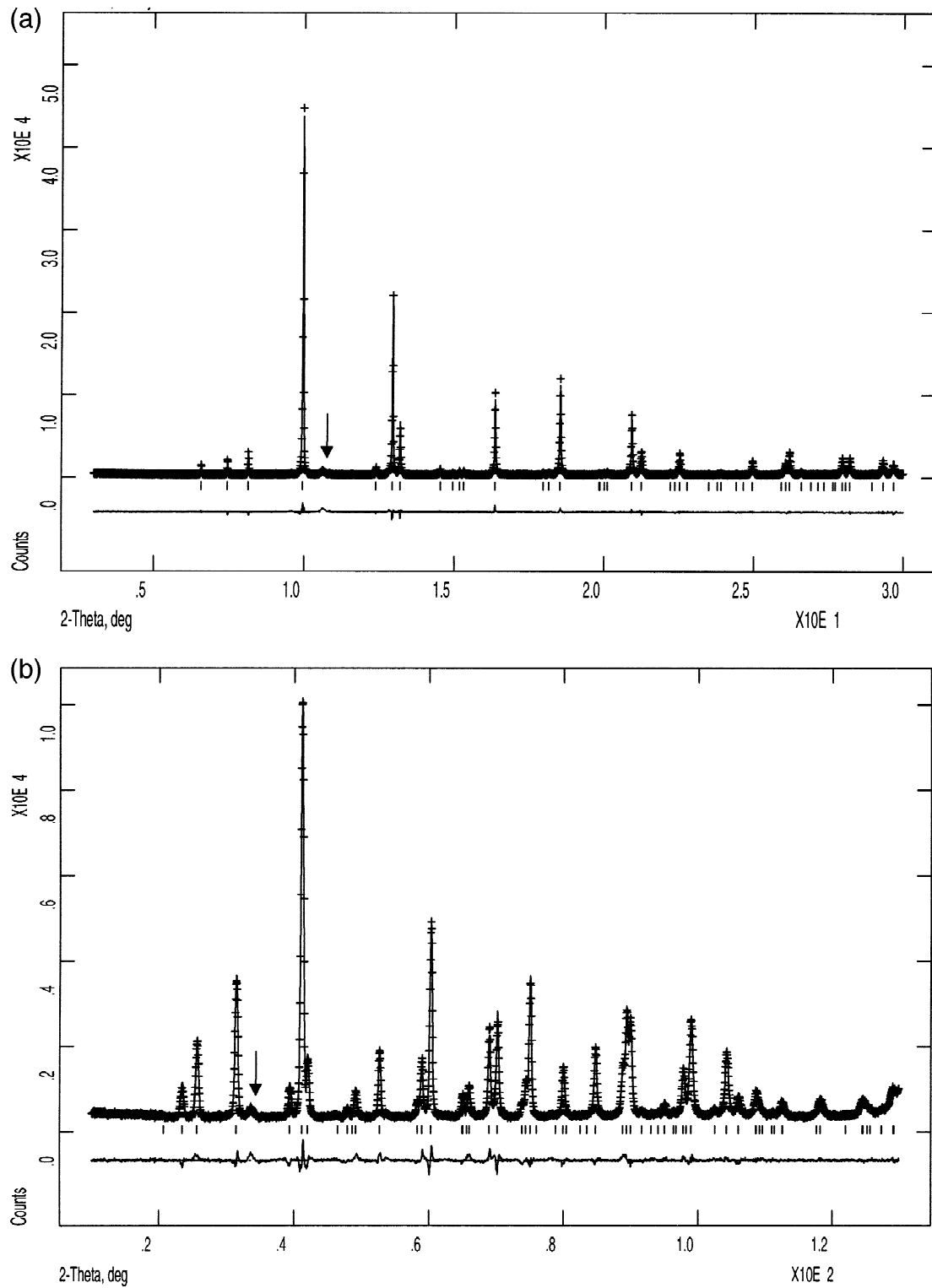


Fig. 1. (a) PXD (SR) and (b) PND patterns for LaNiSnD<sub>2</sub> after combined Rietveld profile refinements showing observed (+), calculated (line) and difference (line at bottom) plots. The peaks marked with arrows at 10.6° (SR XRD) and 33.5° (PND) correspond to the same *d*-spacing of 2.70 Å and belong to an unidentified impurity.

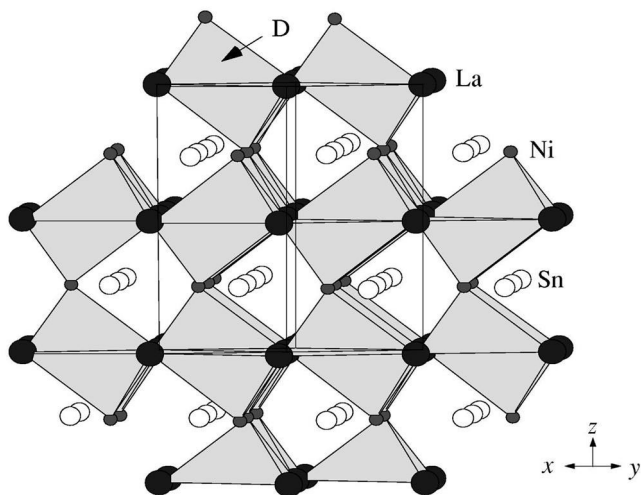


Fig. 2. The crystal structure of  $\text{LaNiSnD}_2$ . The framework of deuterium-occupied  $\text{La}_3\text{Ni}$  tetrahedra connected by vertices and edges is shown.

gives regular  $\text{SnLa}_6$  and  $\text{NiLa}_6$  polyhedra (Fig. 3b and c) and a regular net of hexagonal  $\text{Sn}_3\text{Ni}_3$  (see Fig. 4).

The shortest interatomic distances in the structure are: La–D, 2.6118(5) Å; Ni–D, 1.619(2) Å; Sn–D, 2.718(2) Å; and D–D, 2.780(2) Å.

A characteristic feature of the metal sublattice in both the initial intermetallic compound  $\text{LaNiSn}$  and the deuteride  $\text{LaNiSnD}_2$  is the mutual substitution of Ni and Sn, about 10% for each site, but without deviation from the overall  $\text{LaNiSn}$  stoichiometry.

The influence of tin on the hydrogenation properties seems to be different from the typical ‘blocking’ behaviour characteristic for non-metals. For a nearly completely Sn-filled site, such blocking is observed, with all Sn–D distances exceeding  $\sim 2.7$  Å. However, when tin partially and slightly substitutes Ni in the  $\text{La}_3\text{Ni}$  sites, D-blocking in

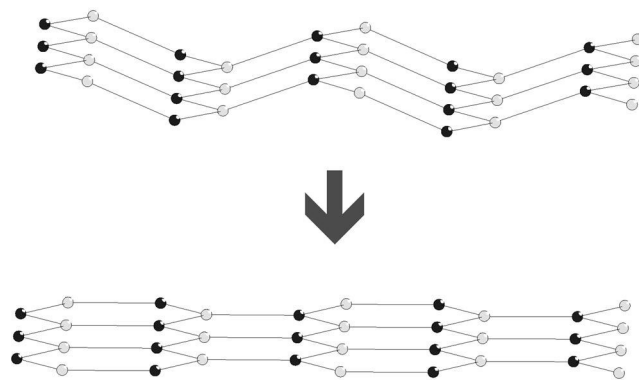


Fig. 4. Change in the Ni–Sn network from  $\text{LaNiSn}$  (top) to  $\text{LaNiSnD}_2$  (bottom). The Ni–Sn planes in  $\text{LaNiSn}$  are buckled, whereas in  $\text{LaNiSnD}_2$  they are regular.

the formed  $\text{La}_3(\text{Ni},\text{Sn})$  interstices does not take place, and the D site is still 100% filled. This specific chemical behaviour of tin may also contribute to the establishment of the advanced properties of Sn-doped  $\text{LaNi}_5$  alloys as H absorbers.

The thermal stability of  $\text{LaNiSnD}_2$  is rather high. Reversible formation of  $\text{LaNiSn}$  from the deuteride proceeds in vacuum at 670 K, with a peak of D evolution at 530–610 K (Fig. 5).

#### Acknowledgements

This work received financial support from Norsk Hydro and the Research Council of Norway. The skillful assistance of the project team at the Swiss–Norwegian Beam Line, ESRF, is gratefully acknowledged. The authors are grateful to R.V. Denys for his help with the preparation of the alloy.

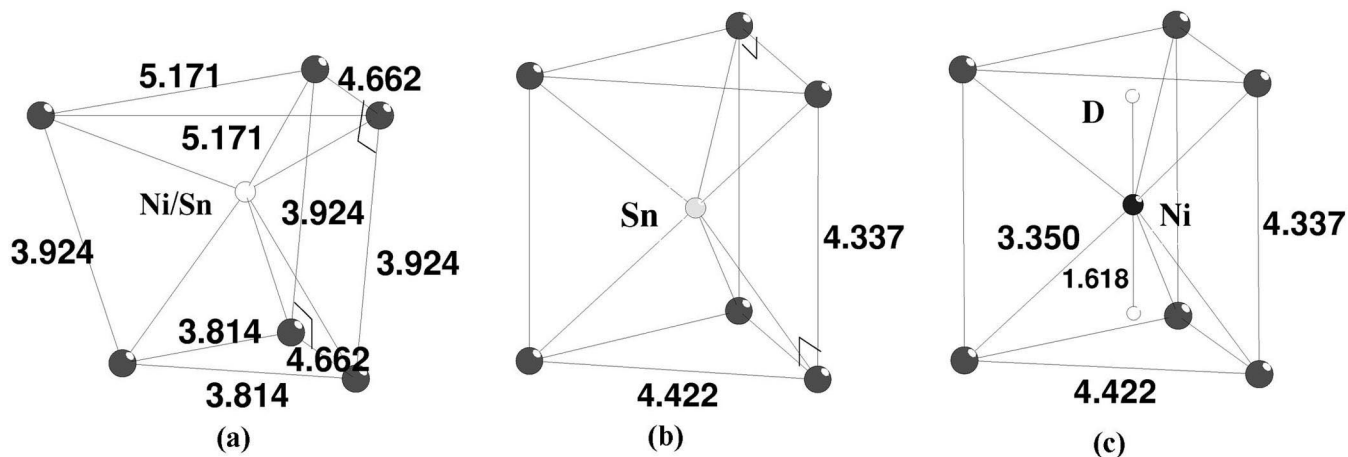


Fig. 3. Change in  $\text{SnLa}_6/\text{NiLa}_6$  polyhedra from  $\text{LaNiSn}$  to  $\text{LaNiSnD}_2$ . La–La distances are marked. (a)  $\text{SnLa}_6/\text{NiLa}_6$  polyhedra in  $\text{LaNiSn}$ . The angles in the upper  $\text{La}_3$  triangle are (from the right) 63.2, 63.2 and 53.6°, and correspondingly 52.3, 52.3 and 75.3° in the lower triangle. The Sn–La distances in the  $\text{SnLa}_6$  polyhedron are 3.24 ( $\times 2$ ), 3.27, 3.33 ( $\times 2$ ) and 3.39 Å and the corresponding La–Ni distances for  $\text{NiLa}_6$  are 3.10, 3.14 ( $\times 2$ ), 3.32 and 3.59 ( $\times 2$ ) Å. (b) Regular  $\text{SnLa}_6$  polyhedron in  $\text{LaNiSnD}_2$ . (c) Regular  $\text{NiLa}_6$  polyhedron in  $\text{LaNiSnD}_2$ . In (b) and (c), all angles in the upper and lower planes are 60° and all Sn/Ni–La distances are 3.35 Å.

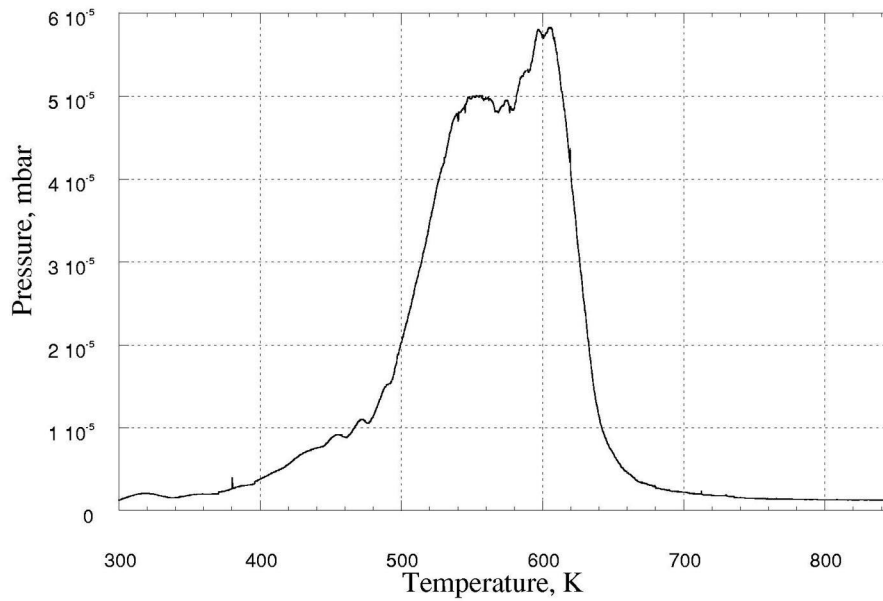


Fig. 5. Vacuum desorption traces of deuterium from  $\text{LaNiSnD}_2$ .

## References

- [1] J.-M. Joubert, M. Latroche, R. Cerný, R.C. Bowman Jr., A. Percheron-Guégan, K. Yvon, *J. Alloys Comp.* 293–295 (1999) 124.
- [2] J.L.C. Daams, K.H.J. Buschow, *Philips J. Res.* 39 (1984) 77.
- [3] A.E. Dwight, *J. Less-Common Met.* 93 (1983) 411.
- [4] R.V. Skolozdra, in: *Handbook on the Physics and Chemistry of Rare Earths*, Vol. 24, 1997, p. 399, Chapter 164.
- [5] A. Szytula (Ed.), *Crystal Structures and Magnetic Properties of RTX Rare Earth Intermetallics*, Jagellonian University Press, Krakow, 1998, p. 82.
- [6] A.C. Larson, R.B. von Dreele, *General Structure Analysis System (GSAS)*. LANSCE, MS-H 805, 1994.